The brain of the silver fox (*Vulpes vulpes*): A neuroanatomical reference of cell-stained histological and MRI images

Christina N. Rogers Flattery[1], **Munawwar Abdulla**[1], **Sophie A. Barton**[1], **Jenny M. Michlich**[2], **Lyudmila N. Trut**[3], **Anna V. Kukekova**[4], **Erin E. Hecht**[1]

[1]Department of Human Evolutionary Biology, Harvard University

[2]Department of Communication Science and Disorders, University of Pittsburgh

[3]The Laboratory of Evolutionary Genetics, Institute of Cytology and Genetics of the Siberian Branch of the Russian Academy of Sciences, Novosibirsk, Russia

[4]Department of Animal Sciences, College of ACES, University of Illinois at Urbana-Champaign

Abstract

Although the silver fox (*Vulpes vulpes*) has been largely overlooked by neuroscientists, it has the potential to serve as a powerful model for the investigation of brain-behavior relationships. The silver fox is a melanistic variant of the red fox. Within this species, the long-running Russian farm-fox experiment has resulted in different strains bred to show divergent behavior. Strains bred for tameness, aggression, or without selection on behavior present an excellent opportunity to investigate neuroanatomical changes underlying behavioral characteristics. Here, we present a histological and MRI neuroanatomical reference of a fox from the conventional strain, which is bred without behavioral selection. This can provide an anatomical basis for future studies of the brains of foxes from this particular experiment, as well as contribute to an understanding of fox brains in general. In addition, this can serve as a resource for comparative neuroscience and investigations into neuroanatomical variation among the family Canidae, the order Carnivora, and mammals more broadly.

Keywords

Canidae; neuroanatomy; Vulpines; brain evolution; comparative neuroscience

Introduction

Atlases are a crucial tool for grounding neuroscience research in a detailed understanding of brain structure. Here, our aim is to provide a preliminary cytoarchitectonic and MRI

anatomical reference dataset of the brain of the silver fox (*Vulpes vulpes*), a species for which there has been genetic and behavioral research (e.g. Woolard and Harris 1990; Trut et al. 2009; Soulsbury 2011; Kukekova et al. 2012, 2018; Henry 2013; Díaz-Ruiz et al. 2016; Wang et al. 2018), but very little neuroanatomical investigation.

The silver fox is a melanistic variant of the red fox (Kukekova et al. 2012). This species belongs to the family Canidae, which also includes gray wolves and domestic dogs. Canid species are only distantly related to other members of the order Carnivora, such as ferrets and domestic cats (Agnarsson et al. 2010; see Figure 1). Nevertheless, canids are of great interest to biologists due to their complex social systems (Kleiman and Eisenberg 1973; Dorning and Harris, 2019), large geographic distribution (Padilla and Hilton, 2015), and high degree of morphological and behavioral diversity (Macdonald and Sillero-Zubiri 2004).

Of all the canid species, the brain of the domestic dog has been studied the most extensively (Ericsson et al. 2013). There are multiple dog brain atlases (Lim et al. 1960; Singer 1962; Palazzi 2011; Datta et al. 2012; Czeibert et al. 2019; Johnson et al. 2020), and a number of structural and functional dog brain studies (e.g. Hecht et al. 2019; Hecht et al. 2021; Andics and Miklósi 2018; Thompkins et al. 2018). By comparison, far less is known about the silver fox brain. To date, only a handful of studies have investigated neuroanatomy in this species (Najdzion et al. 2009; Wasilewska et al. 2012, Huang et al. 2015; Rowniak et al. 2003, 2020, 2022; Hecht et al. 2021; Ortiz-Lea et al. 2022).

Although the silver fox has been largely overlooked by neuroscientists, it has the potential to be a powerful model for the investigation of brain-behavior relationships. For over 60 years, members of this species have been selectively bred in the Russian fox experiment based on their social interactions with humans (Trut et al. 2009; Statham et al. 2011). Three strains have been developed: the tame, aggressive, and conventional strains, originating from populations in Eastern North America (Statham et al., 2011). Unlike wild red foxes, individuals from the tame strain eagerly approach humans and exhibit affiliative behaviors towards them. Meanwhile, foxes from the aggressive strain avoid human contact and are defensively aggressive when approached. Foxes from the conventional strain are kept on the farm but bred without selection on behavior, and are also avoidant of humans (Trut et al. 2009; Statham et al. 2011). Compared to foxes from the tame and aggressive strains, conventional farm-bred foxes although have been bred in captivity for over hundred years, are thought to behave most similarly to wild silver foxes (Trut et al. 2009).

Here, we provide labeled histological sections of a brain from a conventional silver fox from the Russian fox experiment. We also provide a matching MRI section for each histological section. Our hope is that this can serve as an anatomical basis for future studies, both in silver foxes and among strains, as well as bolster comparative research between canid species and other mammals.

Methods

Tissue preparation

Foxes were provided by the Institute of Cytology and Genetics (ICG) of the Russian Academy of Sciences in Novosibirsk, Russia, where the farm-fox experiment has been ongoing since 1959. All animal procedures at the ICG were performed in accordance with standards for humane care and use of laboratory animals by foreign institutions, Office of Laboratory Animal Welfare Assurance F16–00180 (A5761–01). Foxes were euthanized with an intravenous overdose of pharmaceutical grade thiopental sodium immediately before the sample collection at the farm research facility. The use of thiopental sodium for euthanasia is approved by the AVMA Guidelines on Euthanasia. Brain tissue was acquired from 1.5-year old male foxes from the conventional strain, i.e., farmed foxes bred without selection on behavior. Brains were hemisected immediately following extraction. Left hemispheres were prepared by immersion in 10% neutral-buffered formalin and were stored at +4° Celsius for approximately 5 years prior to MRI. Before sectioning, tissue was placed on a rocker in a series of sucrose concentrations: 3 days in 20% sucrose, 3 days in phosphate-buffered saline, 1 day in 10% sucrose, 3 days in 20% sucrose, 1 week in 30% sucrose, 3 weeks in 40% sucrose. Right hemispheres were preserved for other studies and were not available for this endeavor.

Tissue staining

Fixed tissue was sectioned in the coronal plane at 40 μm thickness using a freezing microtome (Thermo Fisher HM450, Waltham, MA). The plane of sectioning was chosen by identifying an imaginary line connecting the anterior and posterior commissures, and sectioning perpendicular to this line. Every 10th section was stained for the Nissl substance with thionin using the following protocol: 3×5 min washes in distilled water (dH2O) were followed by a series of dehydrating alcohol incubations, each for 5 min, in 50%, 70%, 95% (2x), 100% (2x) ethanol. The tissue was then delipidized in xylene twice for 5 min each, followed by a chloroform/xylene incubation for 20 min. The tissue was then once again placed in xylene for 5 min and then rehydrated with another series of alcohol immersions, each for 5 min in 100%, 95%, 70%, and 50% ethanol. Slides were then washed in dH2O for 5 min then placed in a thionin solution (940 mL dH20, 37g sodium acetate, 500 mg thionin acetate, pH to 4.2 with glacial acetic acid) for 7 min, followed by a dH2O rinse and 70% acetic acid for approximately 3 min, 95% ethanol for 1 min, and then 100% ethanol for 2 min. Tissue was moved to an ethanol/xylene solution for 2 min, and 2 xylene incubations for 5 min each, then cover-slipped.

MRI Methods

For scanning, specimens were packaged in a plastic jar and stabilized with polyethylene beads. The jar was then pumped full of Fluorinert FC-770 (3M). Fluorinert is a fluorocarbon which produces no MRI signal and therefore provides a clean background. Images were acquired on a 9.4 T/20 cm horizontal bore Bruker magnet, interfaced to an Avance console, with Paravision 5.1 software (Bruker). A 7.2-cm-diameter volume radio frequency coil was used for transmission and reception. We acquired a RARE T2 sequence (2 averages, 13 ms TE, 2500 ms TR, rare factor 8) at a resolution of 300 μm^3 with a matrix size of 256×100

× 88. Bias correction was accomplished using FAST (Zhang et al., 2001), part of the FSL software package (Smith et al., 2004; Woolrich et al., 2009; Jenkinson et al., 2012). MRI data is displayed mirror-reflected to the histological sections for ease of comparison. MRI data was re-sliced to match the plane of sectioning as closely as possible. Additionally, MRI sections were visually selected to match histological sections as closely as possible.

Digitization and labeling

Stained sections were scanned on an Aperio T2 Whole Slide Scanner (Leica Biosystems, Nussloch, Germany). High quality images at a magnification up to 20x were compared to existing cytoarchitectural atlases and relevant neuroanatomical works to identify and label brain regions. We present every 40th section, cut at 40 μm thick. Thus histological sections are 1.6 mm apart.

Results

Neuroanatomical reference images

Labeled histological images with equivalent MRI sections are provided in PDF format via Supplementary File 1.

Our reference contains 37 plates. Each plate contains a labeled histological section and a matched MRI section, both presented in the coronal plane. Each plate contains a scale bar and key, as well as an indication of the distance in millimeters from the anterior end of the brain. A list of structures is provided in Table 1. Plates 14 and 20 are shown as examples in Figure 2 and Figure 3. Additionally, we provide surface drawings with labels of sulci and gyri (Figure 4).

High-Resolution Digitized Slides

High-resolution scans corresponding to each plate are available at https://dataverse.harvard.edu/dataverse/harvard. Slides can be viewed using ImageScope, free software from Leica Biosystems, available at https://www.leicabiosystems.com/us/digital-pathology/manage/aperio-imagescope/.

MRI Template

Nissl-stained sections are displayed alongside corresponding MRI sections. MRI sections represent the average of 10 1.5-year-old male foxes from the conventional strain, and thus encompass some degree of individual variation present in these animals. The MRI template is available for download as Supplementary File 2.

3D Printable File

We also include a supplementary file in .stl format compatible with 3D printers (Supplementary File 3). This corresponds to the 10-subject average brain template.

List of Structures

Table 1 contains a list of all structures included and associated unique abbreviations.

Discussion

Here, we present a neuroanatomical reference of the left hemisphere of the silver fox (*Vulpes vulpes*). This represents the brain anatomy of the conventional strain from the Russian farm-fox experiment, i.e., farm-raised animals bred without selection on behavior. It should be noted that conventional farm-raised foxes have likely undergone some unintentional behavioral selection as result of living in captivity (Webster and Rutz, 2020; Statham et al., 2011), and the brains of these foxes might therefore differ in some ways from wild foxes. However, the Russian farm-fox experiment represents a well-controlled experimental evolution study where specific selection pressure was applied to behavioral responses in a specific context (i.e., approach by an unfamiliar human), resulting in significant differences in social approach/avoidance behavior in this context. Prior research has examined additional behavioral and physiological traits in these foxes, including HPA-axis and reproductive function (reviewed in Trut et al., 2009; Hekman et al., 2018), intra- and inter-specific communication (Hare et al., 2005; Gogoleva et al., 2008, 2009, 2011), cranial morphology (Kistner et al., 2021), and genomic correlates of behavioral adaptation resulting from experimental selection (Kukekova et al., 2008, 2011a, 2011b, 2018; Nelson et al., 2017; Wang et al., 2018). However, very little neuroscience research has been carried out to date. One study determined that tame foxes show increased adult hippocampal neurogenesis (Huang et al., 2015). Other studies have reported impacts on gene expression and gross morphology in the brain (Kukekova et al., 2011c; Rosenfeld et al., 2020; Hecht et al., 2021a). Because the brain is the intermediate phenotype that links genes to behavior – the ultimate trait under selection in the farm-fox experiment – further research will be necessary to understand how genetic changes produce behavioral changes by affecting brain development, organization, and function. We hope that this reference can provide a foundation for such efforts.

While outside the scope of the present report, this may also be useful for future comparative and evolutionary neuroscience research examining brain organization across related canid and carnivore species. In the absence of an existing fox brain atlas, atlases for closely related species as well as neuroanatomical research articles were compared to our sections to identify brain regions. We compared our sections primarily to dog atlases (Singer 1962; Liu et al. 1960; Palazzi et al. 2011). Gyri and sulci were identified and named following Miller, 1965; Johnson, 2020; and Czeibert, 2018. We also drew from figures in journal articles, particularly for the thalamus (Sakai et al. 1983; Sakai and Smith 1992) and amygdala (Rowniak et al. 2020). Additionally, we drew upon high magnification cat atlases for regions with a large number of small nuclei, such as the brainstem and hypothalamus (Bleier 1961; Snider & Niemer 1961; Berman 1968). There is also an extensive atlas for a wild canid species, the African Wild Dog, which may offer interesting opportunities for comparison (Chengetanai et al., 2020a-d). The current work may also be useful for comparison with more distantly related species. Notably, elaboration and enlargement of the temporal lobe has evolved independently in primates and carnivores (Bryant and Preuss, 2018).

Supplementary Material

Refer to Web version on PubMed Central for supplementary material.

Funding

Data Availability

All data are provided as supplementary files.

References

Agnarsson I, Kuntner M, May-Collado LJ (2010) Dogs, cats, and kin: a molecular species-level phylogeny of Carnivora. Molecular Phylogenetics and Evolution 54:726–745. 10.1016/j.ympev.2009.10.033 [PubMed: 19900567]

Andics A, & Miklósi Á (2018) Neural processes of vocal social perception: Dog-human comparative fMRI studies. Neuroscience & Biobehavioral Reviews 85:54–64. 10.1016/j.neubiorev.2017.11.017 [PubMed: 29287629]

Berman AL (1968) The brain stem of the cat. A cytoarchitectonic atlas with stereotaxic coordinates. University of Wisconsin Press, Madison

Berman AL, Jones EG (1982) The thalamus and basal telencephalon of the cat : a cytoarchitectonic atlas with stereotaxic coordinates. University of Wisconsin Press, Madison.

Bleier R (1961) The Hypothalamus of the Cat: A Cytoarchitectonic Atlas in the Horsley-Clarke Co-ordinate System. Johns Hopkins University Press, Baltimore

Bryant KL and Preuss TM, 2018. A comparative perspective on the human temporal lobe. Digital Endocasts: From skulls to brains, pp.239–258.

Chengetanai S, Tenley JD, Bertelsen MF, Hård T, Bhagwandin A, Haagensen M, Tang CY, Wang VX, Wicinski B, Hof PR and Manger PR, 2020. Brain of the African wild dog. I. Anatomy, architecture, and volumetrics. Journal of Comparative Neurology, 528(18), pp.3245–3261. [PubMed: 32720707]

Chengetanai S, Bhagwandin A, Bertelsen MF, Hård T, Hof PR, Spocter MA and Manger PR, 2020. The brain of the African wild dog. II. The olfactory system. Journal of Comparative Neurology, 528(18), pp.3285–3304. [PubMed: 32798255]

Chengetanai S, Bhagwandin A, Bertelsen MF, Hård T, Hof PR, Spocter MA and Manger PR, 2020. The brain of the African wild dog. III. The auditory system. Journal of Comparative Neurology, 528(18), pp.3229–3244. [PubMed: 32678456]

Chengetanai S, Bhagwandin A, Bertelsen MF, Hård T, Hof PR, Spocter MA and Manger PR, 2020. The brain of the African wild dog. IV. The visual system. Journal of Comparative Neurology, 528(18), pp.3262–3284. [PubMed: 32725830]

Czeibert K, Piotti P, Petneházy Ö, Kubinyi E (2018) Sulci of the canine brain: a review of terminology. bioRxiv 374744. 10.1101/374744

Czeibert K, Andics A, Petneházy Ö, Kubinyi E (2019) A detailed canine brain label map for neuroimaging analysis. Biol. Futura 70:112–120. 10.1556/019.70.2019.14

Díaz-Ruiz F, Caro J, Delibes-Mateos M, Arroyo B, Ferreras P (2015) Drivers of red fox (*Vulpes vulpes*) daily activity: prey availability, human disturbance or habitat structure?. J. Zool 298(2):128–138. 10.1111/jzo.12294

Dorning J, Harris S (2019) Understanding the intricacy of canid social systems: Structure and temporal stability of red fox (*Vulpes vulpes*) groups. PLoS One 14(9):e0220792. 10.1371/journal.pone.0220792 [PubMed: 31509536]

Ericsson AC, Crim MJ, Franklin CL (2013) A brief history of animal modeling. Mo Med 110(3):201–205. [PubMed: 23829102]

Gogoleva SS, Volodin JA, Volodina EV and Trut LN, 2008. To bark or not to bark: vocalizations by red foxes selected for tameness or aggressiveness toward humans. Bioacoustics, 18(2), pp.99–132.

Gogoleva SS, Volodin IA, Volodina EV, Kharlamova AV and Trut LN, 2009. Kind granddaughters of angry grandmothers: the effect of domestication on vocalization in cross-bred silver foxes. Behavioural processes, 81(3), pp.369–375. [PubMed: 19520236]

Gogoleva SS, Volodin IA, Volodina EV, Kharlamova AV and Trut LN, 2011. Explosive vocal activity for attracting human attention is related to domestication in silver fox. Behavioural processes, 86(2), pp.216–221. [PubMed: 21145949]

Hare B, Plyusnina I, Ignacio N, Schepina O, Stepika A, Wrangham R and Trut L, 2005. Social cognitive evolution in captive foxes is a correlated by-product of experimental domestication. Current Biology, 15(3), pp.226–230. [PubMed: 15694305]

Hecht EE, Smaers JB, Dunn WD, Kent M, Preuss TM, Gutman DA (2019) Significant neuroanatomical variation among domestic dog breeds. J Neurosci 39(39):7748–7758. 10.1523/JNEUROSCI.0303-19.2019 [PubMed: 31477568]

Hecht EE, Kukekova AV, Gutman DA, Acland GM, Preuss TM, Trut LN (2021a) Neuromorphological changes following selection for tameness and aggression in the Russian farm-fox experiment. J Neurosci 41(28):6144–6156. 10.1523/JNEUROSCI.3114-20.2021 [PubMed: 34127519]

Hecht EE, Zapata I, Alvarez CE, Gutman DA, Preuss TM, Kent M, Serpell JA (2021b) Neurodevelopmental scaling is a major driver of brain–behavior differences in temperament across dog breeds. Brain Structure and Function 226(8):2725–2739. 10.1007/s00429-021-02368-8 [PubMed: 34455497]

Hekman JP, Johnson JL, Edwards W, Vladimirova AV, Gulevich RG, Ford AL, Kharlamova AV, Herbeck Y, Acland GM, Raetzman LT and Trut LN, 2018. Anterior pituitary transcriptome suggests differences in ACTH release in tame and aggressive foxes. G3: Genes, Genomes, Genetics, 8(3), pp.859–873. [PubMed: 29378821]

Henry JD (1996) Red fox: the catlike canine. Smithsonian Institution, United States

Huang S, Slomianka L, Farmer AJ, Kharlamova AV, Gulevich RG, Herbeck YE, Trut LN, Wolfer DP, Amrein I. Selection for tameness, a key behavioral trait of domestication, increases adult hippocampal neurogenesis in foxes. Hippocampus. 2015 Aug;25(8):963–75. doi: 10.1002/hipo.22420. [PubMed: 25616112]

Johnson PJ, Luh WM, Rivard BC, Graham KL, White A, FitzMaurice M, Loftus JP and Barry EF (2020) Stereotactic cortical atlas of the domestic canine brain. Nature Scientific Reports 10:1–16. 10.1038/s41598-020-61665-0

Kistner TM, Zink KD, Worthington S and Lieberman DE, 2021. Geometric morphometric investigation of craniofacial morphological change in domesticated silver foxes. Scientific Reports, 11(1), p.2582. [PubMed: 33510282]

Kleiman DG, Eisenberg JF (1973) Comparisons of canid and felid social systems from an evolutionary perspective. Anim. Behav 21(4):637–659. 10.1016/s0003-3472(73)80088-0 [PubMed: 4798194]

König JF, Klippel RA (1974). The rat brain : a stereotaxic atlas of the forebrain and lower parts of the brain stem. Robert E. Krieger Publishing Company, Huntington.

Kukekova AV, Temnykh SV, Johnson JL, Trut LN, Acland GM (2011a) Genetics of behavior in the silver fox. Mamm Genome 23:164–177. 10.1007/s00335-011-9373-z [PubMed: 22108806]

Kukekova AV, Trut LN, Chase K, Kharlamova AV, Johnson JL, Temnykh SV, Oskina IN, Gulevich RG, Vladimirova AV, Klebanov S and Shepeleva DV, 2011b. Mapping loci for fox domestication: deconstruction/reconstruction of a behavioral phenotype. Behavior genetics, 41, pp.593–606. [PubMed: 21153916]

Kukekova AV, Johnson JL, Teiling C, Li L, Oskina IN, Kharlamova AV, Gulevich RG, Padte R, Dubreuil MM, Vladimirova AV and Shepeleva DV, 2011c. Sequence comparison of prefrontal cortical brain transcriptome from a tame and an aggressive silver fox (Vulpes vulpes). BMC genomics, 12(1), pp.1–20.

Kukekova AV, Temnykh SV, Johnson JL, Trut LN and Acland GM, 2012. Genetics of behavior in the silver fox. Mammalian genome, 23, pp.164–177. [PubMed: 22108806]

Kukekova AV, Johnson JL, Xiang X, Feng S, Liu S, Rando HM, Kharlamova AV, Herbeck Y, Seryukova NA, Xiong Z, Beklemischeva V, Koepfli KP, Gulevich RG, Vladimirova AV, Hekman JP, Perelman PL, Graphodatsky AS, O'Brien SJ, Wang X, Clark AG, Acland GM, Trut LN, Zhang G (2018) Red fox genome assembly identifies genomic regions associated with tame

and aggressive behaviours. Nat. Ecol. Evol 2:1479–1491. 10.1038/s41559-018-0611-6 [PubMed: 30082739]

Kumar S, Stecher G, Suleski M, Hedges SB (2017) TimeTree: A Resource for Timelines, Timetrees, and Divergence Times. Mol. Biol. Evol 34(7):1812–1819. 10.1093/molbev/msx116 [PubMed: 28387841]

Lim RKS, Liu CN, Moffitt RL (1960) A stereotaxic atlas of the dog's brain. Charles C. Thomas, Springfield.

Macdonald DW, Sillero-Zubiri C (2004) Dramatis personae: an introduction to the wild canids. In: Macdonald DW, Sillero-Zubiri C (ed) Biology and Conservation of Wild Canids, 1st edn. Oxford University Press, Oxford, pp 3–58. 10.1093/acprof:oso/9780198515562.003.0001

Mai JK, Majtanik M, Paxinos G (2015) Atlas Of The Human Brain. Academic Press, Amsterdam.

Miller ME, Christensen GC, Evans HE (1964) Anatomy of the Dog. W.B. Saunders Company, Philadelphia.

Najdzion J, Wasilewska B, Równiak M, Bogus-Nowakowska K, Szteyn S, Robak A. A morphometric comparative study of the medial geniculate body of the rabbit and the fox. Anat Histol Embryol. 2011 Oct;40(5):326–34. doi: 10.1111/j.1439-0264.2011.01076.x. [PubMed: 21539595]

Nelson RM, Temnykh SV, Johnson JL, Kharlamova AV, Vladimirova AV, Gulevich RG, Shepeleva DV, Oskina IN, Acland GM, Rönnegård L and Trut LN, 2017. Genetics of interactive behavior in silver foxes (Vulpes vulpes). Behavior genetics, 47, pp.88–101. [PubMed: 27757730]

Ortiz-Leal I, Torres MV, Villamayor PR, Fidalgo LE, López-Beceiro A, Sanchez-Quinteiro P (2022) Can domestication shape canidae brain morphology? The accessory olfactory bulb of the red fox as a case in point. Ann. Anat 240:151881. 10.1016/j.aanat.2021.151881 [PubMed: 34896556]

Padilla LR, Hilton CD (2015) Canidae. Fowler's Zoo and Wild Animal Medicine 8(8):457–467. 10.1016/B978-1-4557-7397-8.00046-3

Palazzi X (2011) The beagle brain in stereotaxic coordinates. In The Beagle Brain in Stereotaxic Coordinates. Springer, New York, pp1–115.

Paxinos G (1999) Chemoarchitectonic atlas of the rat forebrain. Academic Press, San Diego.

Paxinos G, Watson C (2009). Chemoarchitectonic atlas of the mouse brain. Elsevier, Amsterdam.

Paxinos G, Franklin KBJ (2019) The mouse brain in stereotaxic coordinates. London; San Diego; Cambridge; Kidlington, Academic Press, San Diego, Cambridge, Kidlington, Oxford.

Paxinos G, Watson C (2013). The rat brain in stereotaxic coordinates. Academic Press, San Diego.

Popova NK, Voitenko NN, Kulikov AV, Avgustinovich DF (1991) Evidence for the involvement of central serotonin in mechanism of domestication of silver foxes. Pharmacol Biochem Behav 40(4):751–756. 10.1016/0091-3057(91)90080-l [PubMed: 1816562]

Popova NK, Voitenko NN, Trut LN (1976) Changes in the content of serotonin and 5-hydroxyindoleacetic acid in the brain in the selection of silver foxes according to behavior. Neurosci. Behav. Physiol 7(1):72–74. 10.1007/bf01148752 [PubMed: 1036195]

Popova NK, Kulikov AV, Avgustinovich DF, Voĭtenko NN, Trut LN (1997) Vliianie domestikatsii serebristo-chernykh lists na osnovnye fermenty metabolizma serotonina i serotoninovye retseptory [Effect of domestication of the silver fox on the main enzymes of serotonin metabolism and serotonin receptors]. Genetika 33(3):370–374. [PubMed: 9244768]

Radtke-Schuller S (2018) Cyto- and myeloarchitectural brain atlas of the ferret (Mustela putorius) in MRI aided stereotaxic coordinates. Springer, Cham.

Rosenfeld CS, Hekman JP, Johnson JL, Lyu Z, Ortega MT, Joshi T, Mao J, Vladimirova AV, Gulevich RG, Kharlamova AV and Acland GM, 2020. Hypothalamic transcriptome of tame and aggressive silver foxes (Vulpes vulpes) identifies gene expression differences shared across brain regions. Genes, Brain and Behavior, 19(1), p.e12614. [PubMed: 31605445]

Równiak M, Bogus-Nowakowska K, Kalinowski D, Kozłowska A. The evolutionary trajectories of the individual amygdala nuclei in the common shrew, guinea pig, rabbit, fox and pig: A consequence of embryological fate and mosaic-like evolution. J Anat. 2022 Mar;240(3):489–502. doi: 10.1111/joa.13571. [PubMed: 34648181]

Równiak M, Szteyn S, Robak A. A comparative study of the mammalian amygdala: a Golgi study of the basolateral amygdala. Folia Morphol (Warsz).

Równiak M, Bogus-Nowakowska K (2020) The amygdala of the common shrew, guinea pig, rabbit, fox and pig: five flavours of the mammalian amygdala as a consequence of clade-specific mosaic-like evolution. J. Anat 236(5):891–905. 10.1111/joa.13148 [PubMed: 31898329]

Sakai ST, Smith A (1992) Distribution of nigrothalamic projections in the dog. J. Comp. Neurol 318(1):83–92. 10.1002/cne.903180106 [PubMed: 1583156]

Sakai ST, Stanton GB, Tanaka D Jr (1983) The ventral lateral thalamic nucleus in the dog: Cytoarchitecture, acetylthiocholinesterase histochemistry, and cerebellar afferents. Brain Res 271(1):1–9. 10.1016/0006-8993(83)91359-8 [PubMed: 6883107]

Singer M (1962) The brain of the dog in section. W.B. Saunders Company, Philadelphia.

Snider RS, Niemer WT (1961) A stereotaxic atlas of the cat brain. University of Chicago Press, Chicago.

Soulsbury CD, Iossa G, Baker PJ, White PC, Harris S (2011) Behavioral and spatial analysis of extraterritorial movements in red foxes (Vulpes vulpes). J. Mammal 92(1):190–199. 10.1644/09-MAMM-A-187.1

Statham MJ, Trut LN, Sacks BN, Kharlamova AV, Oskina IN, Gulevich RG, Johnson JL, Temnykh SV, Acland GM, Kukekova AV, (2011) On the origin of a domesticated species: identifying the parent population of Russian silver foxes (Vulpes vulpes). Biol. J. Linn. Soc. Lond 103(1):168–175. 10.1111/j.1095-8312.2011.01629.x [PubMed: 21625363]

Stelmasiak M, Sta ski F (1956). Anatomical atlas of the human brain and spinal cord. Polish State Medical Publishers, Warsaw.

Thompkins AM, Ramaiahgari B, Zhao S, Gotoor SSR, Waggoner P, Denney TS, Deshpande G, Katz JS (2018) Separate brain areas for processing human and dog faces as revealed by awake fMRI in dogs (Canis familiaris). Learning & Behavior, 46:561–573. 10.3758/s13420-018-0352-z [PubMed: 30349971]

Trut L, Oskina I, Kharlamova A (2009) Animal evolution during domestication: the domesticated fox as a model. Bioessays 31(3):349–360. 10.1002/bies.200800070 [PubMed: 19260016]

Wang X, Pipes L, Trut LN, Herbeck Y, Vladimirova AV, Gulevich RG, Kharlamova AV, Johnson JL, Acland GM, Kukekova AV, Clark AG (2018). Genomic responses to selection for tame/aggressive behaviors in the silver fox (Vulpes vulpes). Proc. Natl. Acad. Sci. U.S.A 115(41):10398–10403. 10.1073/pnas.1800889115 [PubMed: 30228118]

Wasilewska Barbara, Najdzion Janusz, Równiak Maciej, Bogus-Nowakowska Krystyna, Nowakowski Jacek J. and Robak Anna. "Morphometric Comparative Study of the Striatum and Globus Pallidus of the Common Shrew, Bank Vole, Rabbit, and Fox" Journal of Veterinary Research, vol.56, no.3, 2012, pp.411–414. 10.2478/v10213-012-0072-7

Webster MM and Rutz C, 2020. How STRANGE are your study animals?. Nature, 582(7812), pp.337–340. [PubMed: 32541916]

Woollard T, Harris S (1990) A behavioural comparison of dispersing and non-dispersing foxes (Vulpes vulpes) and an evaluation of some dispersal hypotheses. J Anim Ecol 59(2):709–722. 10.2307/4890

Zyleger S, Staubesand J (1977) Atlas of the central nervous system in sectional planes: Selected myelin stained sections of the human brain and spinal cord. Urban And Schwarzenberg, Baltimore.
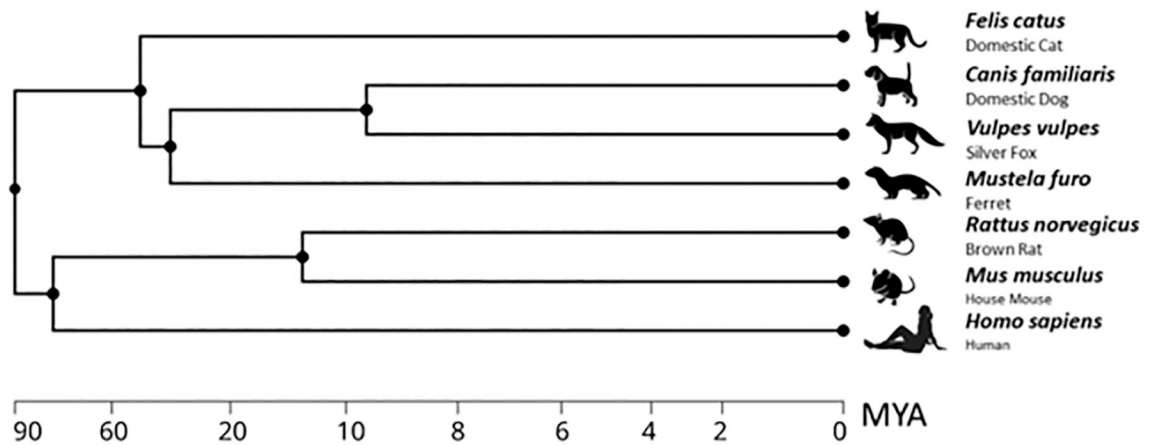
Figure 1:

Phylogenetic tree showing the evolutionary relationship between *Vulpes vulpes* and other species of interest to neuroscience, including other canids (such as *Canis familiaris*), other members of the family Carnivora (such as *Felis cactus* and *Mustela furo*), rodents (such as common animal model species *Mus musculus* and *Rattus norvegicus*), and primates (such as *Homo sapiens*). While there is no previously existing neuroanatomical reference for *Vulpes vulpes*, brain atlases exist for *Felis catus* (Berman 1968; Berman and Smith 1982; Snider and Niemer 1987), *Canis familiaris* (Lim et al. 1960; Singer 1962; Miller et al. 1964; Palazzi 2011), *Mustela furo* (Radtke-Schuller 2018), *Rattus norvegicus* (König and Klippel 1974; Paxinos 1999; Paxinos and Watson 2018), *Mus musculus* (Paxinos and Watson 2009; Paxinos and Franklin 2019), and *Homo sapiens* (Stelmasiak and Sta ski 1956; Zyleger and Staubesand 1977; Mai et al. 2015). Phylogenetic tree constructed using the *TimeTree* resource (Kumar et al. 2017).

Key

AEG = Anterior ectosylvian gyrus
AES = Anterior ectosylvian sulcus
AnS = Ansate sulcus
AS = Septal area
ASSG = Anterior suprasylvian gyrus
ASSS = Anterior suprasylvian sulcus
ASyG = Anterior sylvian gyrus
BST = Bed nucleus of the stria terminalis
BL = Basolateral nucleus of the amygdala
BM = Basomedial nucleus of the amygdala
cc = Corpus callosum
Cd = Caudate nucleus
CE = Central nucleus of the amygdala
CG = Cingulate gyrus
Cl = Claustrum
CO = Cortical nucleus of the amygdala
Cs = Coronal sulcus
En = Entopeduncular nucleus
f = Fornix
Gp = Globus pallidus
Hla = Lateral hypothalamic area
ic = Internal capsule
In = Infundibulum
LA = Lateral nucleus of the amygdala

ME = Medial nucleus of the amygdala
MG = Marginal gyrus
opt = Optic tract
Pa = Paraventricular nucleus of the hypothalamus
Pir = Piriform cortex
PCG = Postcruciate gyrus
Pu = Putamen
R = Reticular nucleus of the thalamus
Rhf = Rhinal fissure
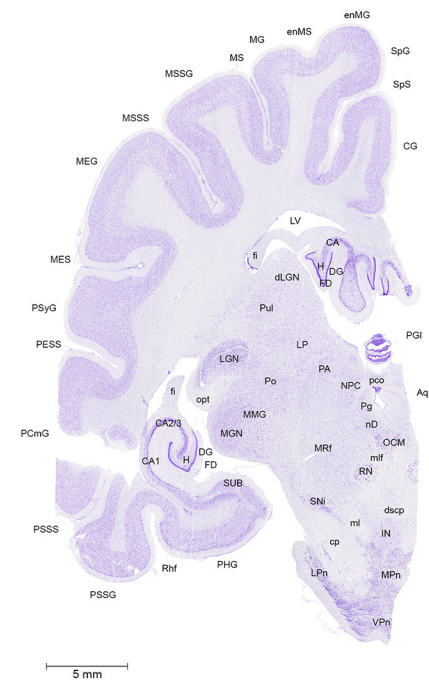SpS = Splenial sulcus
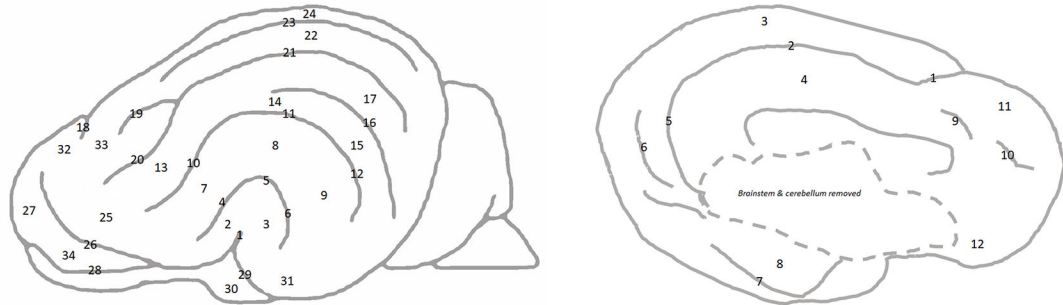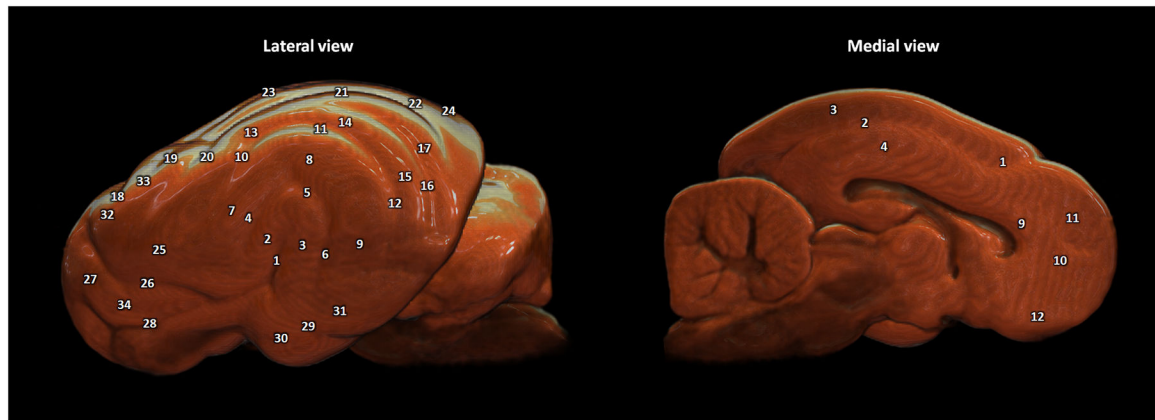Vem = Ventromedial nucleus of the hypothalamus

Figure 2:
Plate 14.

Key

Aq = Cerebral aqueduct
CA1 = Cornu ammonis field 1 of the hippocampus
CA2/3 = Cornu ammonis field 2/3 of the hippocampus
CG = Cingulate gyrus
cp = Cerebral peduncle
DG = Dentate gyrus of the hippocampus
dLGN = Dorsal lateral geniculate nucleus
dscp = Decussation of the superior cerebellar peduncle
enMG = Endomarginal gyrus
enMS = Endomarginal sulcus
FD = Fascia dentata
fi = fimbria
H = Hilus
IN = Interpeduncular nucleus
LGN = Lateral geniculate nucleus
LP = Lateral posterior nucleus of the thalamus
LPn = Lateral pontine nuclei
LV = Lateral ventricle
MEG = Medial ectosylvian gyrus
MES = Medial ectosylvian sulcus
MG = Marginal gyrus
MGN = Medial geniculate nucleus
ml = Medial lemniscus
mlf = Medial longitudinal fasciculus
MMG = Magnocellular nucleus of medial geniculate body
MPn = Medial pontine nuclei
MRf = Midbrain reticular formation

MS = Marginal sulcus
MSSG = Medial suprasylvian gyrus
MSSS = Medial suprasylvian sulcus
nD = Nucleus of Darkschewitsch
NPC = Nucleus of the posterior commissure
OCM = Oculomotor nucleus
opt = Optic tract
PA = Pretectal area
PCmG = Composite gyrus
pco = Posterior commissure
PESS = Posterior ectosylvian sulcus
Pg = Periaqueductal gray
PGl = Pineal gland
PHG = Parahippocampal gyrus
Po = Posterior nucleus of the thalamus
PSSG = Posterior suprasylvian gyrus
PSSS = Posterior suprasylvian sulcus
PSyG = Posterior sylvian gyrus
Pul = Pulvinar
Rhf = Rhinal fissure
RN = Red nucleus
SNi = Substantia nigra
SpG = Splenial gyrus
SpS = Splenial sulcus
SUB = Subiculum
VPn = Ventral pontine nuclei

Figure 3:
Plate 20.

1: Pseudosylvian fissure	12: Posterior suprasylvian sulcus	23: Endomarginal sulcus	1: Cruciate sulcus
2: Anterior sylvian gyrus	13: Anterior suprasylvian gyrus	24: Endomarginal gyrus	2: Splenial sulcus
3: Posterior sylvian gyrus	14: Middle suprasylvian gyrus	25: Anterior composite gyrus	3: Splenial gyrus
4. Anterior ectosylvian sulcus	15: Posterior suprasylvian gyrus	26: Presylvian sulcus	4: Cingulate gyrus
5: Middle ectosylvian sulcus	16: Ectomarginal sulcus	27: Prorean gyrus	5: Retrosplenial sulcus
6: Posterior ectosylvian sulcus	17: Ectomarginal gyrus	28: Anterior part of lateral rhinal sulcus	6: Occipitotemporal sulcus
7: Anterior ectosylvian gyrus	18: Cruciate sulcus	29: Posterior part of lateral rhinal sulcus	7: Posterior rhinal fissure
8: Middle ectosylvian gyrus	19: Ansate sulcus	30: Piriform lobe	8: Piriform lobe
9: Posterior ectosylvian gyrus	20: Coronal sulcus	31: Posterior composite gyrus	9: Genual sulcus
10: Anterior suprasylvian sulcus	21: Marginal sulcus	32: Precruciate gyrus	10: Rostral sulcus
11: Middle suprasylvian sulcus	22: Marginal gyrus	33: Postcruciate gyrus	11: Frontal gyrus
		34: Orbital gyrus	12: Straight gyrus

Figure 4:

Schematic drawing of cortical surface with labels for sulci and gyri.

Table 1:

Labeled brain structures and unique abbreviations.

3V	Third ventricle
ac	Anterior commissure
ACmG	Anterior composite gyrus
aCN	Accessory cuneate nucleus
AD	Anterior dorsal nucleus of the thalamus
AEG	Anterior ectosylvian gyrus
AES	Anterior ectosylvian sulcus
AFL	Ansiform lobule
AM	Anterior medial nucleus of the thalamus
AmN	Ambiguous nucleus
AN	Abducens nucleus
AnS	Ansate sulcus
AON	Anterior olfactory nucleus
Aq	Cerebral aqueduct
AS	Septal area
ASSG	Anterior suprasylvian gyrus
ASSS	Anterior suprasylvian sulcus
ASyG	Anterior sylvian gyrus
AV	Anterior ventral nucleus of the thalamus
bic	Brachium of the inferior colliculus
BL	Basolateral nucleus of the amygdala
BM	Basomedial nucleus of the amygdala
BST	Bed nucleus of the stria terminalis
CA1	Cornu ammonis field 1 of the hippocampus
CA2	Cornu ammonis field 2 of the hippocampus
CA3	Cornu ammonis field 3 of the hippocampus
cc	Corpus callosum
Cc	Central lobule of the cerebellum
Cd	Caudate nucleus
CE	Central nucleus of the amygdala
CeP	Cerebellar peduncle
Cg	Coronal gyrus
CG	Cingulate gyrus
Cl	Claustrum
CLN	Centrolateral nucleus
CN	Cochlear nucleus
cn5	Trigeminal nerve
cn7	Facial nerve
cn8	Cranial nerve
CnC	Central canal

CM	Centromedian thalamic nucleus
CO	Cortical nucleus of the amygdala
cp	Cerebral peduncle
CPRN	Caudal pontine reticular nucleus
Cs	Coronal sulcus
CS	Cruciate sulcus
csc	Commissure of the superior colliculus
Cu	Cuneiform nucleus
Cuc	Culmen of the cerebellum
CuN	Cuneate nucleus
Db	Diagonal band of Broca
Dc	Declive of the cerebellum
Den	Dentate nucleus of the cerebellum
DG	Dentate gyrus of the hippocampus
dLGN	Dorsal lateral geniculate nucleus
Dm	Dorsomedial nucleus of the hypothalamus
dpt	Decussation of the pyramidal tract
DR	Dorsal raphe
dscp	Decussation of the superior cerebellar peduncle
DVN	Dorsal vagal nucleus
ecMG	Ectomarginal gyrus
ecMS	Ectomarginal sulcus
En	Entopeduncular nucleus
enMG	Endomarginal gyrus
enMS	Endomarginal sulcus
f	Fornix
FD	Fascia dentata
FF	Nucleus of the fields of forel
FG	Frontal gyrus
fi	Fimbria
FL	Flocculus
FMN	Facial motor nucleus
Fn	Fastigial nucleus of the cerebellum
Gi	Gigantocellular reticular nucleus
GN	Gracile nucleus
Gp	Globus pallidus
Gr	Gyrus rectus
Gs	Genual sulcus
H	Hilus of the hippocampus
Haa	Anterior hypothalamic area
Hda	Dorsal hypothalamic area
Hgn	Hypoglossal nucleus
Hla	Lateral hypothalamic area

Hpa	Posterior hypothalamic area
ic	Internal capsule
icc	Inferior colliculus commissure
ICN	Nucleus of the inferior colliculus
icp	Inferior cerebellar peduncle
In	Infundibulum
IN	Interpeduncular nucleus
INn	Interposed nucleus of the cerebellum
ION	Inferior olivary nucleus
IsC	Islands of Calleja
ITP	Bed nucleus of the inferior thalamic peduncle
LA	Lateral nucleus of the amygdala
Lc	Lingula of the cerebellum
LC	Locus coeruleus
LD	Lateral dorsal nucleus of thalamus
LGN	Lateral geniculate nucleus
LH	Lateral habenula
ll	Lateral lemniscus
lot	Lateral olfactory tract
LP	Lateral posterior nucleus of the thalamus
LPn	Lateral pontine nuclei
LRN	Lateral reticular nucleus
LS	Lateral septum
LV	Lateral ventricle
mcp	Medial cerebellar peduncle
MD	Mediodorsal nucleus of the thalamus
ME	Medial nucleus of the amygdala
MEG	Medial ectosylvian gyrus
MES	Medial ectosylvian sulcus
MG	Marginal gyrus
MGN	Medial geniculate nucleus
MH	Medial habenula
ml	Medial lemniscus
mlf	Medial longitudinal fasciculus
Mm	Mammillary body
MMG	Magnocellular nucleus of medial geniculate body
MnV	Trigeminal motor nucleus
MOBgl	Main olfactory bulb, glomerular layer
MOBgr	Main olfactory bulb, granule layer
MOBopl	Main olfactory bulb, outer plexiform layer

MOB mi	Main olfactory bulb, mitral layer
MPn	Medial pontine nuclei
MR	Median raphe
MRf	Midbrain reticular formation
MS	Marginal sulcus
Ms	Medial septum
MSSG	Medial suprasylvian gyrus
MSSS	Medial suprasylvian sulcus
mtt	Mammillothalamic tract
MV	Medioventral nucleus of the thalamus
NAc	Nucleus accumbens
Nbic	Nucleus of the brachium of the inferior colliculus
Nc	Nodulus of the cerebellum
nD	Nucleus of Darkschewitsch
NPC	Nucleus of the posterior commissure
nST	Nucleus of the solitary tract
Ntb	Nucleus of the trapezoid body
OCM	Oculomotor nucleus
OPRn	Oral pontine reticular nucleus
opt	Optic tract
OS	Olfactory sulcus
OT	Olfactory tubercle
OTS	Occipitotemporal sulcus
ox	Optic chiasm
Pa	Paraventricular nucleus of the hypothalamus
PA	Pretectal area
PAT	Parataenial nucleus of the thalamus
PBB	Pontobulbar body
Pc	Pyramis of the cerebellum
PC	Paracentral nucleus of the thalamus
PCG	Postcruciate gyrus
PCmG	Posterior composite gyrus
pco	Posterior commissure
PCS	Postcruciate sulcus
Pe	Periventricular nucleus of the hypothalamus
Pea	Anterior periventricular nucleus of the hypothalamus
PEG	Posterior ectosylvian gyrus
PESS	Posterior ectosylvian sulcus
Pf	Parafascicular nucleus of the thalamus
PFL	Paraflocculus
Pg	Periaqueductal gray

PG	Prorean gyrus
PGl	Pineal gland
PHG	Parahippocampal gyrus
Pir	Piriform cortex
PML	Paramedian lobule
Pn	Pontine nuclei
Po	Posterior nucleus of the thalamus
PrCG	Precruciate gyrus
PRN	Parvocellular reticular nucleus
Ps	Presylvian sulcus
PS	Prorean sulcus
PSG	Posterior sylvian gyrus (not sigmoid!)
PSSG	Posterior suprasylvian gyrus
PSSS	Posterior suprasylvian sulcus
PSyG	Posterior sylvian gyrus
pt	Pyramidal tract
Pu	Putamen
Pul	Pulvinar
R	Reticular nucleus of the thalamus
Rf	Reticular formation
Rh	Rhomboid nucleus
Rhf	Rhinal fissure
Rn	Reuniens nucleus of the thalamus
RN	Red nucleus
Rs	Rostral sulcus
rSpS	Retrosplenial sulcus
RTN	Reticulotegmental nucleus
SC	Superior colliculus
scp	Superior cerebellar peduncle
Sg	Suprageniculate nucleus
SI	Substantia innominata
Smn	Supramammillary nucleus
SMT	Stria medullaris terminalis
SNi	Substantia nigra
SnV	Sensory nucleus of trigeminal nerve
So	Supraoptic nucleus of the hypothalamus
SON	Supraolivary nucleus
SpG	Splenial gyrus
SpS	Splenial sulcus
SpV	Spinal trigeminal nucleus
SS	Sylvian sulcus
SSG	Suprasylvian gyrus
SSpG	Suprasplenial gyrus

SSpS	Suprasplenial sulcus
SSS	Suprasylvian sulcus
St	Nucleus of the stria terminalis
Stn	Subthalamic nucleus
SUB	Subiculum
SuG	Subcallosal gyrus
SVZ	Subventricular zone
tb	Trapezoid body
Tc	Tuber of the cerebellum
Tca	Tuber cinereum area
tst	Tectospinal tract
Uc	Uvula of the cerebellum
VA	Ventroanterior nucleus
Vem	Ventromedial nucleus of the hypothalamus
VL	Ventrolateral nucleus
VM	Ventroposteromedial nucleus
VNI	Inferior vestibular nucleus
VNL	Lateral vestibular nucleus
VNLL	Ventral nucleus of the lateral lemniscus
VNM	Medial vestibular nucleus
VPL	Ventral posterior lateral thalamic nucleus
VPn	Ventral pontine nuclei
VRN	Ventral reticular nucleus
VTA	Ventral tegmental area
ZI	Zona incerta